Journal of Materials Science: Materials in Medicine (2020)31:22
https://doi.org/10.1007/s10856-020-6361-4

BIOCOMPATIBILITY STUDIES

Original Research

β-cyclodextrin coating: improving biocompatibility of magnetic nanocomposites for biomedical applications

Mariela Agotegaray[1] · María Gabriela Blanco[2] · Adrián Campelo[3] · Elba García[1] · Roberto Zysler[4] · Virginia Massheimer[3] · María José De Rosa[2] · Verónica Lassalle[1]

Received: 30 May 2019 / Accepted: 8 January 2020

Abstract

The role Beta-cyclodextrin (βCD) on improving biocompatibility on healthy cellular and animal models was studied upon a formulation obtained from the development of a simple coating procedure. The obtained nanosystems were thoroughly characterized by FTIR, TGA, atomic absorption spectroscopy, dynamic light scattering and zeta potential, TEM/HR-TEM and magnetic properties. βCD might interact with the magnetic core through hosting OA. It is feasible that the nanocomposite is formed by nanoparticles of MG@OA dispersed in a βCD matrix. The evaluation of βCD role on biocompatibility was performed on two healthy models. To this end, in vivo studies were carried out on *Caenorhabditis elegans*. Locomotion and progeny were evaluated after exposure animals to MG, MG@OA, and MG@OA-βCD (10 to 500 μg/mL). The influence of βCD on cytotoxicity was explored in vitro on healthy rat aortic endothelial cells, avoiding alteration in the results derived from the use of transformed cell lines. Biological studies demonstrated that βCD attaching improves MG biocompatibility.

Graphical Abstract

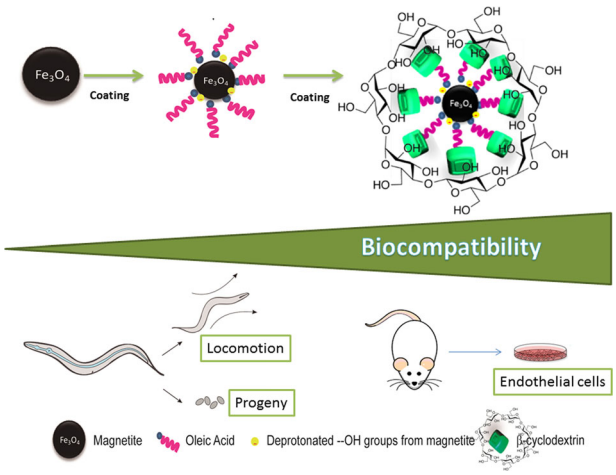

Supplementary information The online version of this article (https://doi.org/10.1007/s10856-020-6361-4) contains supplementary material, which is available to authorized users.

✉ Mariela Agotegaray
magotegaray@uns.edu.ar

✉ María José De Rosa
mjderosa@criba.edu.ar

[1] Departamento de Química, Instituto de Química del Sur (INQUISUR-CONICET)-UNS, Universidad Nacional del Sur, Bahía Blanca, Argentina

[2] Dpto. de Biología, Bioquímica y Farmacia, Instituto de Investigaciones Bioquímicas de Bahía Blanca (INIBIBB-CONICET)-UNS, Lab. de Neurobiología de Invertebrados, Universidad Nacional del Sur, Bahía Blanca, Argentina

[3] Dpto. de Biología, Bioquímica y Farmacia,Instituto de Investigaciones Biológicas y Biomédicas del Sur (INBIOSUR-CONICET)-UNS, Universidad Nacional del Sur, Bahía Blanca, Argentina

[4] CONICET—Centro Atómico Bariloche, Instituto Balseiro, S.C. de Bariloche, Río Negro, Argentina

Published online: 30 January 2020

1 Introduction

The emergence of magnetic nanomaterials applicable in biomedicine has led to extensive research on the development of new nanosystems based on magnetic iron oxide nanoparticles (MNPs) [1]. They find applications in diverse fields such as transport and drug targeting [2], treatment of oncological diseases by hyperthermia [3], and diagnosis by magnetic resonance imaging [4]. When the development of nanomaterials is oriented to biomedicine, it is fundamental to consider the toxicological aspects. In this way, the design and development of nanosystems with a biocompatible coating is mandatory.

There is a variety of coatings for MNPs [5]. Several works have been devoted to the study of β-cyclodextrin (βCD) as coating for nanoparticles [6–13]. The methods described for the attachment of βCD to MNPs are, in general, based on derivatization of the side hydroxyl groups of βCD to bind the magnetic core, leading to a great number of steps during synthesis. In addition, the use of harmful and pollutant organic solvents during the synthesis turns these procedures difficult to scale up to concrete production for biomedical approaches.

The present work aims to use a different strategy on MNPs coating with βCD, to avoid long-time and multiple-step procedures. A very simple and effective method is proposed, consisting in the attachment of βCD through its inner cavity to oleic acid (OA) tails from OA-coated iron oxide MNPs, by means of hydrophobic interactions. Hydroxyl-exposed groups from βCD could thus be available for further modification with the desired bioactive drugs or molecules for magnetic drug targeting.

A novel aspect that we address in this work is related with the evaluation of βCD-functionalized MNPs toxicity on healthy models. Reported studies related to the cytotoxicity of magnetic nanosystems functionalized with βCD are all based on in vitro experiments in tumor cell cultures, namely human cervical cancer cells (HeLa) [6–12], human breast cancer cell lines (MDA-MB-231) [12], and human epidermoid carcinoma cells (A431) [8]. It is worthy of note that our work on biocompatibility was carried out in primary cultures of endothelial cells (ECs), thus avoiding alteration in the results derived from the use of transformed cell lines. ECs form a monolayer lining the entire vascular system. They were chosen to carry out cytotoxicity studies because of their critical role in the regulation of the exchange of biomolecules between bloodstream and surrounding tissues.

On the other hand, we used the model *Caenorhabditis elegans* to evaluate the biocompatibility of these nanocomposites in a living organism. *C. elegans* is a stablished model for toxicological studies [13, 14]. *C. elegans* is easy to grow and culture in the laboratory and it has a short life cycle. This therefore guarantees a rapid and low cost efficient evaluation of toxicological features of drugs and/or materials in the context of a whole animal. However, there are no previous reports in this or other animal models involving the effect of βCD coating on the toxicity of MNPs. The use of invertebrate animals as platform to study toxicity of nanomaterials is currently a novel tool that will allow carrying out further studies in mammals with the support of toxicological screening [15, 16]. The aim of implementing this kind of model is reducing the number of mammalian animals used. This is in line with Bioethics and significantly reduces expenses and assay time.

Summing up, this work presents a different and simple way to attach βCD to MNPs to obtain magnetic nanocomposites with improved biocompatibility as platform for the incorporation of drugs for magnetic targeting.

2 Experimental

2.1 Materials and methods

2.1.1 Procedure to obtain the nanocomposites

The preparation was conducted in two steps. The first one consisted in obtaining of magnetite nanoparticles (MG) functionalized with oleic acid (OA) by co-precipitation: 20 mL of an aqueous mixture containing $FeSO_4 \cdot 7H_2O$, $FeCl_3 \cdot 6H_2O$ in (Fe^{2+}/Fe^{3+}) molar ratio equal to 0.5 and 0.3 g of OA was added dropwise with 5 mL of NaOH 5 M under nitrogen atmosphere and magnetic stirring at 70 °C. The obtained dispersion was cooled until room temperature, separated by a Nd magnet and washed with distilled water. This procedure was repeated three times to ensure a suitable elimination of the oleic acid excess. The sample was dried at 45 °C.

Coating with βCD consisted in dispersing MG@OA MNPs (0.5 mg/mL) in hexane under ultrasound during 15 min (See Figure S1 in Electronic Supplementary Information). Then, an aqueous solution of βCD was added to the former dispersion and the mixture was kept for 24 h under vigorous magnetic stirring. The influence of βCD concentration was studied by exploring concentrations of 1.25, 2.50, and 5.00 mM. After reaction, the organic phase was discarded and the resulting nanocomposites were purified from the aqueous phase by magnetic decantation and by washing with distilled water. The resulting formulations are hereafter named MG@OA-βCD1, MG@OA-βCD2, MG@OA-βCD3 that respectively indicate increases in βCD concentration during synthesis.

3 Characterization

Fourier transform infrared spectroscopy (FTIR) was performed using a Thermo Scientific Nicolet 6700 spectrometer.

Spectra were recorded in the range 4000–400 cm^{-1}. Samples were prepared dispersing the corresponding solid in KBr to obtain pellets of 1% concentration.

Thermogravimetric analyses (TGA) were performed on a SDT Q600 Universal TA Instrument. MG, MG@OA, MG@OA-βCD1, and MG@OA-βCD2 were weighted and heated from room temperature to 650 °C under air atmosphere with a heating rate of 10 °C/min.

The iron content of all magnetic samples was determined by atomic absorption spectroscopy using a GBC Avanta 932 spectrometer. Samples were prepared by dissolving 10 mg of magnetic nanoparticles in 10 mL HCl 36% w/v, and by preparing dissolutions as necessary.

Transmission electron microscopy (TEM, JEOL 100 CX II, Tokyo, Japan from CCT, Bahía Blanca, Argentina) and high-resolution TEM (Phillips CM200 UT microscope operating at 200 kV) were used to examine the morphology of nanocomposites. Samples for TEM analysis were dispersed in water at a concentration of 0.1 mg/mL. A drop of this suspension was placed on a 200 mesh carbon-coated copper grid and dried at room temperature.

Z potential measurements and hydrodynamic diameter of MNPs were measured using a Malvern Zetasizer (Nano-Zs90). Samples for Z potential determination were prepared as aqueous dispersions of MNPs employing distilled water at a concentration of 0.1 mg/mL. Dispersions with the same concentration of MG@OA were prepared in hexane, and dispersions with concentrations of MG@OA-βCD1, MG@OA-βCD2, and MG@OA-βCD3 were prepared in distilled water. The average particle hydrodynamic diameter was determined after ultrasonication during 30 min.

Magnetic properties were measured with a commercial vibrating sample magnetometer (VSM) at room temperature (RT) scanning a magnetic field in the 10 to +10 kOe range. The sample (powder) was weighted and subsequently placed in the sampler unit for measurement.

3.1 Evaluation of biocompatibility on C. elegans

3.1.1 *C. elegans* culture and maintenance

Worms were cultured and maintained on *Escherichia coli* OP50 lawns on Nematode Growth Medium (NGM) agar plates, according to standard protocols at 20 °C [17, 18]. For all experiments, animals were synchronized by leaving gravid adults for 6–8 h and then removing them and keeping the eggs. After 3 days, young adult population was used for different assays. *C. elegans* Bristol strain N2 and *E. coli* OP50 were obtained from *Caenorhabditis Genetic Center* (CGC), University of Minnesota, St. Paul, MN, USA.

L4 larvae/young adult worms were exposed to different samples (MG, MG@OA, and MG@OA-βCD2 magnetic nanocomposite). As a control, animals were incubated in Milli-Q water.

Worms were exposed to nanocomposites in liquid media. Under this condition animals are forced to swim and continuously absorb the dispersed particles. Milli-Q water was used because other standard *C. elegans* buffers as M9 may promote aggregation of nanocomposites [19]. Incubation was carried out under rotating agitation and in absence of food to ensure homogeneous contact between animals and particles.

3.1.2 Biodistribution assay

Adult worms were treated with MG, MG@OA, and the βCD functionalized magnetic nanocomposite at concentrations from 10 to 500 μg/mL for 24 h. They were subsequently fixed with 4% paraformaldehyde during 2 h at RT. Fixed worms were washed three times with Milli-Q water and stained with a mixture of Perl´s solution (4% KFeCN/4% HCl) incubated in the dark for 1 h and washed three times. Worms were then mounted on a glass slide and observed under a Nikon Eclipse TE 2000 S microscope. The assay was repeated three times. At least 20 worms were used for each condition in each independent experiment.

3.1.3 Thrashing assay

It is a well-established method for measuring motility in *C. elegans*. To investigate the effects of MG, MG@OA and MG@OA-βCD2 on motor behavior, thrashing rates were evaluated as the frequency of thrashes for 60 s under a microscope. Worms were incubated for 24 h at different doses of the formulations under study (0–500 μg/mL). Then, the magnetic samples were removed and worms were transferred to a multi-well plate containing M9 (one worm/well) and were left to wait for ~10 min before starting the assay. A minimum of 12 worms were counted for each experimental condition. Experiments were conducted at least 3 times. The mean thrashing count ± SE for each group was evaluated.

3.1.4 Progeny score

Worms were exposed for 24 h to MG, MG@OA, and MG@OA-βCD2 at the mentioned concentrations in Milli-Q water and were subsequently transferred to a NGM plate with food. The number of progeny was scored after 72 h. The experiments were repeated in triplicate in three independent worm preparations.

3.2 Evaluation of toxicity on endothelial cells

The protocols employed for this study have been approved by the Institutional Committee for the Care and Use of

Experimental Animals belonging to BBF-UNS, in accordance to the internationally accepted standard Guide for the Care and Use of Laboratory Animals as adopted and promulgated by the National Institute of Health [19].

3.3 Effects on endothelial cell culture

Primary cultures of ECs were obtained from aortic ring explants isolated from young Wistar rats [20].

3.4 Endothelial cell viability assay

Endothelial cell viability was measured by the MTT assay (Sigma-Aldrich). Cells were seeded onto 96 well plates (1×10^4 cells per well) and incubated for 24 h in 100 µl of DMEM with 2% FCS. Cells were treated with different concentrations of the magnetic formulations or vehicle alone for 48 h. After treatment, 10 µl of MTT reagent were added to each sample and the plate was incubated in darkness at 37 °C under a 5% CO_2 atmosphere for 4 h. After incubation, the medium was removed and 100 µl of DMSO were added to each well. The absorbance was measured at 550 nm in a multiplate reader (Biotek Synergy-HT) using 690 nm as the reference. Results are expressed as optical density (OD).

3.5 Statistical analysis

For the biocompatibility assays, statistical significance between control and treated groups was assessed using one-way ANOVA followed by Holm–Sidak tests.

4 Results

4.1 Synthesis and physicochemical characterization

The procedure to obtain nanocomposites rendered three formulations depending on MG@OA:βCD ratios.

FTIR spectra (Fig. 1a, b) of OA-coated MNPs, raw βCD, and the three magnetic formulations obtained, are presented in Fig. 1 to demonstrate the efficient grafting of βCD on MNPs surface.

TGA analysis not only provides information on the composition of the magnetic nanocomposites but also reinforces the qualitative data provided by FTIR spectroscopy. TGA was performed on MG, MG@OA, MG@OA-βCD1, and MG@OA-βCD2. Thermograms are shown in Figure S2 (please see Supplementary Material) and the corresponding results are listed in Table 1.

A decrease in iron content was evidenced comparing bare MG with MG@OA, MG@OA-βCD1, and MG@OA-βCD2. This indicated that the organic layer composed of OA and βCD surrounding the magnetic core was denser, which was consistent with TGA. The increase in βCD concentration in synthesis led to an increase in the coating layer. The organic layer was estimated in 8% for MG@OA-βCD1 and in 15% for MG@OA-βCD2.

Determination of iron content on the samples was used as a complement of TGA data to estimate the composition of MNPs. The results obtained in terms of MG % content are listed in Table 1.

Results on the hydrodynamic diameter and zeta potential measurements for each nano-system in aqueous medium (pH 6.00) are shown in Table 1. The hydrodynamic diameter regarding MG@OA dispersed in hexane resulted as 340.0 ± 10.0 nm with a polydispersion index (PDI) of 0.391. These values are lower in comparison to the formulation dispersed in water as solvent.

Figure 2a–c shows TEM images for the three samples composed of OA and βCD-grafted magnetite. The spherical shape of the magnetic core is observed before and after the reaction with βCD. Magnetic core shows a diameter of ~10 nm. The increase of βCD initial concentration during synthesis renders less aggregated nanocomposites, thus indicating better dispersion. HR-TEM micrograph (Fig. 3d) shows the lattice pattern corresponding to the spinel cubic structure characteristic of magnetite. The magnetic core of the composite, as evidenced in the micrograph, presents crystalline planes with a single orientation for each one, which is ascribable to the single-crystal nature of the nanoparticles [20].

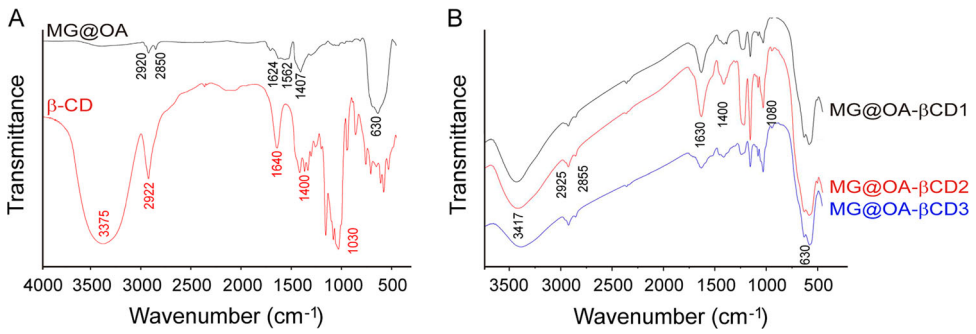

Fig. 1 FTIR spectra of MG@OA and βCD **a** and of the three formulations of magnetic nanocomposites of MG@OA and βCD, obtained from different nominal initial concentration of the oligosaccharide used in the synthesis procedure **b**

Table 1 Results and analysis based on TGA curves of the samples studied; hydrodynamic diameter and zeta potential for each formulation obtained

Sample	First weight loss		Second weight loss		Third weight loss		Total weight loss	MG[a] (%)	Dh[b]/ nm (PDI)	ζ[b] / mV
–	Derivative peak (°C)	Weight loss (%)	Derivative peak (°C)	Weight loss (%)	Derivative peak (°C)	Weight loss (%)	–			
MG	55	5.40	–	–	–	–	5.40	90.0	1300.0 ± 150.0 (0.167)	−26.0 ± 4.3
MG@OA	75	4.34	280	4.90	–	–	9.24	84.0	772.0 ± 12.0 (0.560)	−14.7 ± 5.2
MG@OA-βCD1	60	3.70	275	5.62	430	2.60	11.90	75.0	589.3 ± 42.7 (0.380)	2.3 ± 6.1
MG@OA-βCD2	50	5.50	240–300	10.60	420	4.40	20.50	69.7	370.3 ± 6.0 (0.390)	10.3 ± 4.8
MG@OA-βCD3	–	–	–	–	–	–	–	–	555.4 ± 8.5 (0.456)	14.4 ± 5.1

[a]Calculated through iron determination by atomic absorption spectroscopy

[b]Measured in aqueous dispersions at pH = 6.00. The data reported are the average of three measurements

4.2 Biocompatibility in C. elegans

After exposure to the formulations and aiming to ensure that the absorption of the nanocomposites readily occurs in *C. elegans*, particle incorporation and biodistribution were evaluated by staining the iron-containing magnetic component using Perl´s Prussian Blue colorant. After administration of MG, MG@OA, and MG@OA-βCD2 at different concentrations (0–500 µg/mL), 100% of animals resulted stained. Stained nanocompounds were located in the gut, indicating that they entered to the animal body mainly by ingestion (Fig. 3). The MG@OA-βCD nanocomposites were retained mainly in the intestine. Vulva diffusion, which is another entry pathway [21], was not observed in our study.

Locomotor behavior (movement) of *C. elegans* is useful in assessing toxicity [22]. Swimming velocity (number of thrashes/min) was used to quantify worm locomotion [23]. Similarly to other reports [24], we categorized motility into two groups according to the response against treatment. One group was categorized as "low mobility" (L) which includes those animals presenting slow movements (~20% of regular number of thrashes, from 0 to 50). The other group was categorized as "normal mobility" (N) and includes the animals which presented middle and normal motility (from 50 to 300 thrashes) after treatment.

Both groups showed no statistical differences between control (water-treated) and all MNPs treated-worms from 10 to 100 µg/mL doses (Fig. 4a). At higher concentrations (500 µg/mL), only MG induced a significant effect. Animals under this treatment, exhibited an important impairment in their movement. Under this condition, "L" group represented the main motility group (reaching 79%, 15-fold larger than control condition that reached only 5%). In agreement, the effect of the treatment with bare nano MG, MG@OA, and MG@OA-βCD2 on progeny, the analysis of brood size indicated that at low concentrations (10–100 µg/mL) none of the magnetic nanosystems tested affected progeny. No statistical differences between control and treated-worms were observed (Fig. 4b). At 500 µg/mL dose, only MG-treated group showed a significant decrease in the number of progeny, being ~30% of the control progeny (Fig. 4b).

4.3 Cytotoxicity on rat aortic endothelial cells

Aiming to contribute on the knowledge about the biocompatibility on normal cells of magnetic systems containing β-CDs, rat aortic endothelial cells (ECs) were employed considering that the endothelium is the first barrier that MNPs face before arriving to tissues and organs when they are intended for biomedical applications.

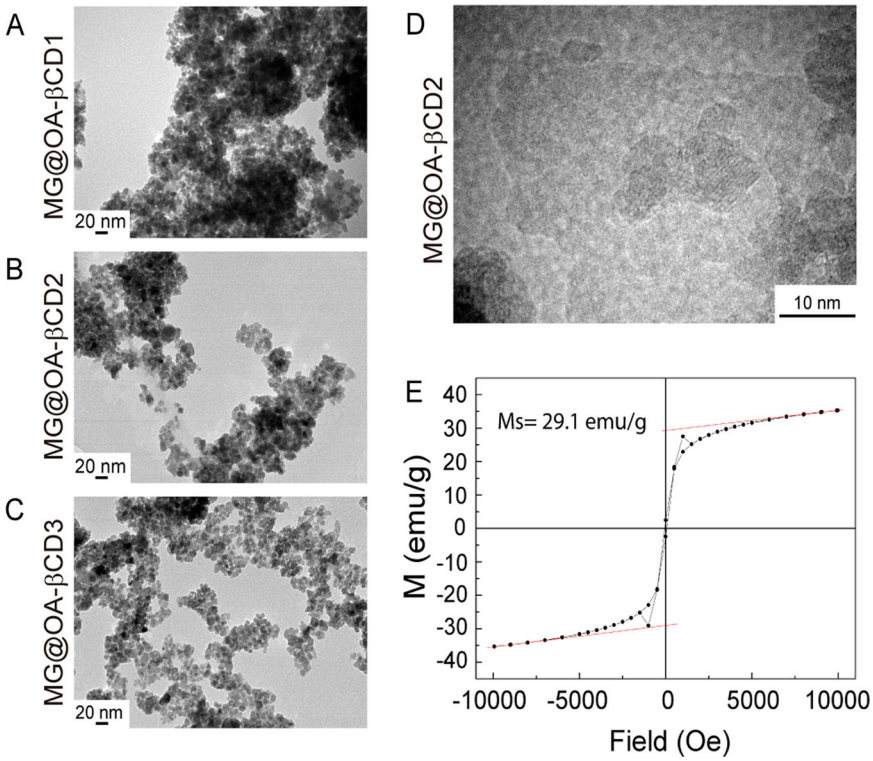

Fig. 2 **a**–**c** TEM micrographs obtained from dried aqueous dispersions of MG@OA-βCD1, MG@OA-βCD2, and MG@OA-βCD3, respectively. **d** HR-TEM micrograph corresponding to MG@OA-βCD2. **e** Magnetization (M) vs. magnetic field (H) curve corresponding to MG@OA-βCD2 at room temperature

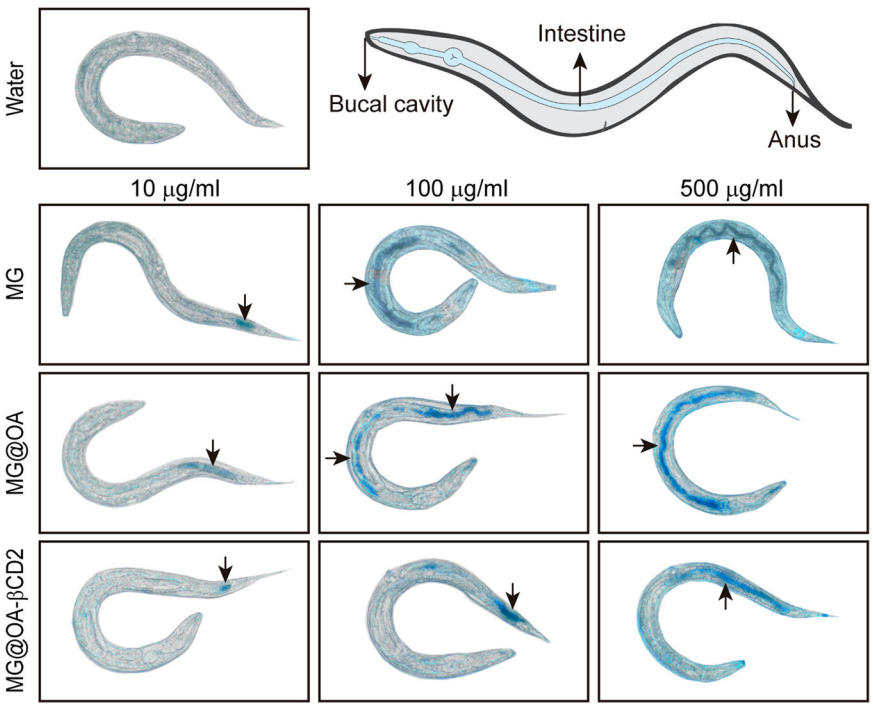

Fig. 3 Perls' Prussian Blue staining of young adult *C. elegans* after exposure to different concentrations (0–500 μg/mL) of MG, MG@AO, and MG@AO-βCD2 for 24 h. Arrows indicate the presence of MNPs evidenced through blue stained iron, mainly in the gut

Figure 5 shows results on ECs viability exposed to different concentrations (1, 10, 100, and 500 μg/mL) of MG@OA-βCD2 for 24 h. Tetrazolium dye (MTT) assay was performed on ECs to analyze cell viability after 24 h of treatment.

5 Discussion

The preparation methodology involved the dispersion of MG@OA in hexane because its hydrophobic nature restricts its dispersion in aqueous medium. When OA is used as a

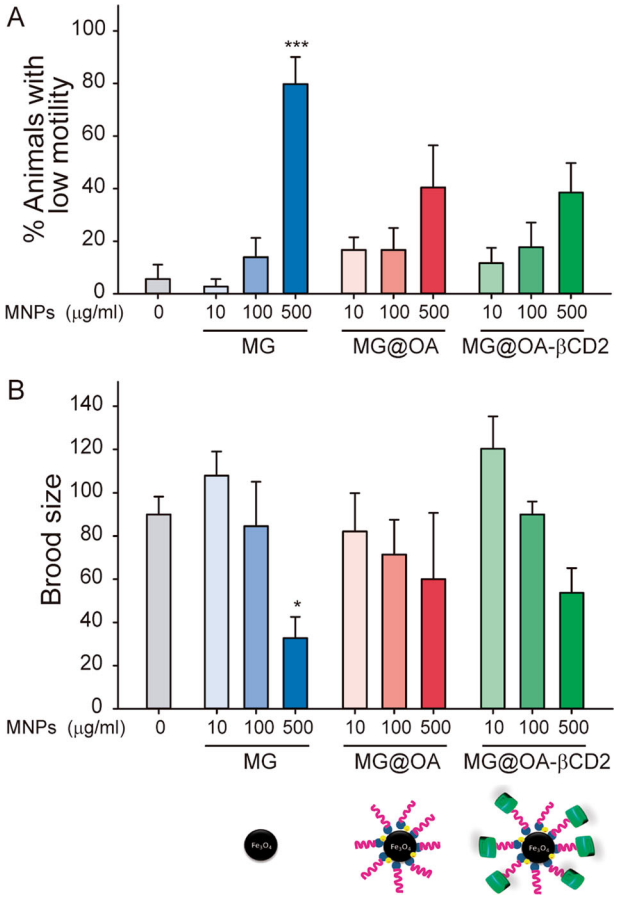

Fig. 4 Evaluation of biocompatibility in *C. elegans*. Worms were exposed to different concentrations (0–500 μg/mL) of MG, MG@AO MG@OA, and MG@AO-□ MG@OA-βCD2 CD2 in water for 24 h. **a** Percentage of worms with low motility (<50 body bends per min) after treatment. **b** To evaluate the brood size, treated young adults were transferred to NGM plates seeded with OP50 and progeny was scored after 72 h. Significant differences were only observed in worms exposed to MG 500 μg/mL. Data are expressed as mean ± SEM ($n = 3$), $*p < 0.05$, $***p < 0.001$

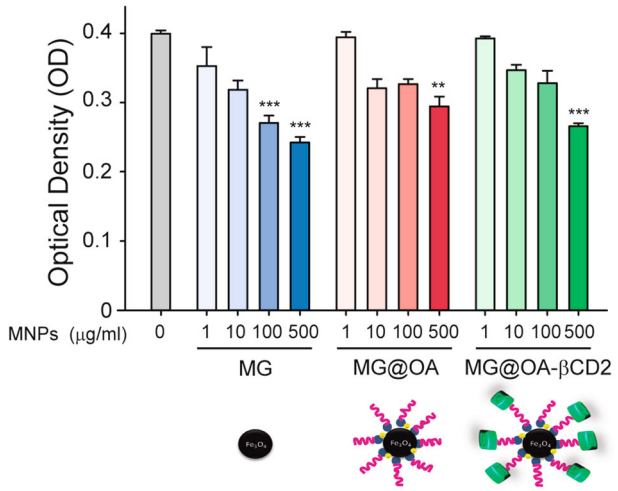

Fig. 5 Viability of endothelial cells incubated with MG@OA-βCD at different concentrations in comparison to control. Cells were exposed to 1, 10, and 100 μg/mL of MNPs for 24 h. Data are expressed as mean ± S.D. $*p < 0.01$ vs. control. At least three independent experiments were analyzed

functionalizing agent for bare MG, it might interact as a mono or a bilayer [25]. This property is very important in the present work: a monolayer coating is necessary to facilitate the non-polar interactions with βCD to obtain a successful grafting. Their efficient dispersion in hexane, as a previous step for synthesis, was an indicator of OA-MG functionalizing as monolayer. The transfer of the MNPs obtained from hexane to the aqueous phase predicted a successful coating with βCD considering its hydrophilicity (Fig. S1). Further characterization, explained below, confirms this hypothesis.

The spectrum of MG@OA MNPs displays a band located near 630 nm due to Fe–O stretching vibration of Fe_3O_4. The presence of OA bands is also observed, indicating its effective incorporation on the iron oxide core surface through the synthesis procedure applied. Pure OA presents two sharp bands at 2924 and 2854 cm^{-1} ascribable to the asymmetric CH_2 stretching vibration and to the symmetric CH_2 stretching, respectively. An intense peak at 1710 cm^{-1} is due to the C=O stretching vibration and the signal at 1285 cm^{-1} is attributable to the C–O stretch. Two other bands at 1462 and 937 cm^{-1} correspond to O–H vibrations in-plane and out-of-plane, respectively [26]. In the spectrum of MG@OA MNPs, two bands at 2920 and 2850 cm^{-1}, are observed, which are shifted to lower wavenumbers in comparison to the pure OA spectrum. This shifting of symmetric and asymmetric stretching vibration of CH_2 group, indicates that hydrocarbon chains from OA surround the magnetic core forming a closed-pack crystalline state [23]. The wavenumber separation (Δ) between the asymmetric and symmetric stretching vibration bands of carboxylate group is a useful parameter to elucidate the type of interaction that occurs between the carboxylate and the metal atom. It is established that Δ lower than 110 cm^{-1} corresponds to chelating bidentate interaction [27]. In this case, the separation is 62 cm^{-1} so a chelating bidentate covalent linkage occurs between COO^- from OA and Fe corresponding to Fe_3O_4 MNPs. The absence of the band near 1710 cm^{-1} is indicative of coating as monolayer [25]. This observation is consistent with the inefficient dispersion of MG@OA in aqueous medium.

βCD spectrum presents an intense band at 3375 cm^{-1} assignable to O–H stretching vibrations. The band located at 2922 cm^{-1} is ascribable to asymmetric and symmetric stretching vibrations of C–H. The band located at 1640 cm^{-1} is characterized by the presence of H–O–H deformation signals corresponding to water associated to βCD. The group of bands located between 1200 and 1400 cm^{-1} is due to C–C stretching vibrations. The intense bands located near

1030 cm^{-1} are due to C–H and C–O stretching vibrations [27]. IR spectra corresponding to MNPs functionalized with βCD present clear bands corresponding to the oligosaccharide: the band located at 3417 cm^{-1} is assignable to O–H stretching vibration although it is noteworthy that this band is absent in the MG@OA spectrum. The signals at 2925 and 2855 cm^{-1} are attributable to asymmetric and symmetric C–H vibrations of both βCD and OA. Bands described for pure βCD are shifted in the spectrum of the three nano-magnetic formulations, ensuring a successful functionalization.

All samples evidenced weight loss at a temperature lower than 100 °C, which was ascribable to water loss. MG@OA samples suffered from one weight loss at ~280 °C which was associated to OA degradation. The thermal degradation of free OA was found to begin at 140 °C and to end below 500 °C [28]. The existence of one process for thermal degradation of OA may indicate that OA coating consists in a single layer in which COO^- group binds Fe from MG in a unique manner [25, 26]. The composition of the organic phase for MG@OA was estimated in ~9.3%. MG@OA-βCD1 underwent four thermal degradation processes. The first was observed to be associated to water loss but it was extended to 118 °C in comparison to MG and MG@OA. This behavior may correspond to the loss of water from the inner cavity of βCD [29]. The following processes are ascribable to degradation of both OA and βCD. The first one occurred at ~270 °C in coincidence with degradation of OA and the second one, which occurred at 430 °C, could be due to decomposition of macrocycles from βCD [30]. In the case of MG@OA-βCD2, a thermal degradation pattern similar to that in MG@OA-βCD1 was observed, but weight loss was higher. Results derived from TGA indicate that organic composition of MG@OA was ~4.9%, ~8.3% for MG@OA-βCD1 and 15.0% for MG@OA-βCD2. This is consistent with the initial concentrations of βCD used during synthesis.

Taken together, results from the physicochemical phenomena observed during synthesis, FTIR spectroscopy, TGA, and iron content determination all confirm coating with βCD on MG@OA. Coating was denser when the initial concentration of βCD was increased.

The polydispersion indexes found for aqueous dispersions of βCD-coated MNPs indicate that samples are almost monodispersed. This behavior shows that the three synthesis conditions with different βCD concentrations facilitate coating, enabling hydrophilic interactions with water molecules. Negative zeta potential value for MG@OA is due to deprotonated hydroxyl groups of magnetite that are exposed to the surface. Considering that OA interacts with MG through carboxylate groups as shown by FTIR data, the concentration used for OA may not be enough to coat all sites in magnetite, therefore, the negative surface charge is justified [26].

DLS measurements reveal that the formulation obtained using the lowest βCD nominal concentration shows the highest hydrodynamic diameter in aqueous medium, in coincidence with TEM micrographs where agglomeration is observed. This behavior in aqueous medium is ascribable to an insufficient βCD concentration to ensure a complete grafting. Even though the amount of βCD attached is enough to increase surface zeta potential in comparison to MG@OA, it is not enough to prevent aggregation due to the possible exposure of the non-polar tail. The results collected in terms of hydrodynamic diameter regarding MG@OA dispersed in water (Table 1) and hexane, size and PDI are higher in comparison to the formulation dispersed in organic medium. This reinforces the evidence of OA coating as a monolayer. The tendency of MG@OA to aggregate itself into the aqueous medium is possibly due to the non-polar tail from OA. The increase in βCD initial concentration during synthesis augmented not only the hydrodynamic size but also the zeta potential for MG@OA-βCD2 and MG@OA-βCD3. The mechanism associated to this trend lies in the amount of βCD attached to the MNPs. The increase in zeta potential values is consistent with an increased number of βCD molecules interacting with the OA hydrophobic tail, which hide the negative hydroxyl groups exposed from magnetite. This leads to higher zeta potential values when initial concentration of βCD is higher. The increment of βCD prevents agglomeration from aqueous insolubility of the exposed OA tail. Scheme 1 shows the structures proposed for MG@OA-βCD1, MG@OA-βCD2, and MG@OA-βCD3.

For biological applications, nanocomposites are expected not to exceed 500 nm in diameter for drug targeting because they can be probably captured by reticuloendothelial system (RES) in liver, diminishing blood circulation time. On the other hand, neutral NPs may be the most proper because they avoid RES capture due to a decrease in opsonisation [31]. In this respect, both MG@OA-βCD1 and MG@OA-βCD2 exhibit almost neutral surface charge (2 and 10 mV, respectively).

MG@OA-βCD2 presents a correct balance among size, surface charge and βCD coating to be applied as a nanocarrier in biomedicine. This formulation was selected to assess toxicological effects in in vitro and in vivo assays. The evaluation of superparamagnetism is mandatory for biomedical applications. The analysis of the magnetization curve included in Fig. 2e for MG@OA-βCD2 indicates that this nanosystem is superparamagnetic. M(H) curve is reversible, with a saturation magnetization Ms = 29.1 emu/g. This value is satisfactory for magnetic targeting on biomedical applications [31]. Magnetization saturation values lower than 70 emu/g and 50 emu/g were previously obtained in our laboratory for MG and MG@OA [32]. Bare

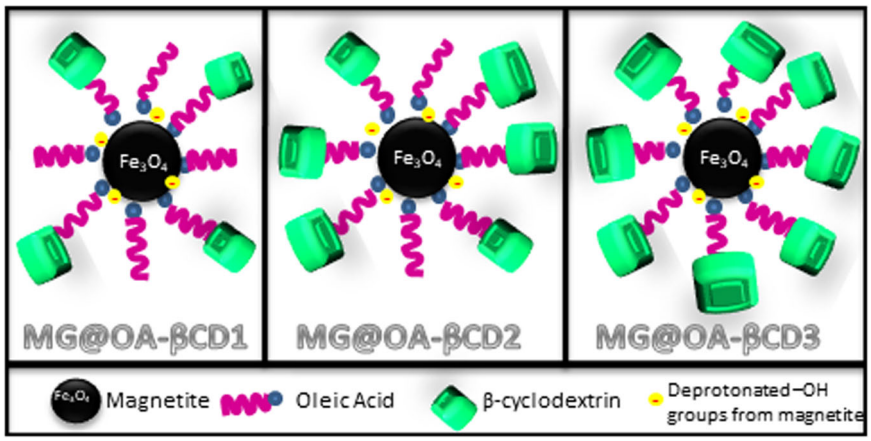

Scheme 1 Structures proposed for MG@OA-βCD1, MG@OA-βCD2, and MG@OA-βCD3

MG nanoparticles were observed to exhibit a high value of magnetization saturation, although the saturation magnetization value was usually reduced in nanoscale due to coating [33]. The results obtained for MG@OA-βCD2 are in agreement with this evidence.

Studies of the toxicity exerted by nanocomposites involving multi-cellular organisms are scarce. The effect of attaching βCD to MNPs on biocompatibility was analyzed in *C. elegans*. It is a useful model to study toxicity of diverse materials and drugs, representing a valuable model to predict animal toxicity. The main advantages of this model are: (1) its high homology to mammal genes and (2) the feasibility of performing rapid assays [13]. It has two sex forms, as hermaphrodite or as a male. The self-fertile is the predominant adult form. At 20 °C hermaphrodites usually lay 300–350 eggs and once the eggs hatch it takes about three days to develop from larva to adult (Figure S2, Electronic Supplementary Information). *C. elegans* has a transparent and simple intestinal system (with mild acidic media and digestive enzymes). This facilitates the detection of modifications in nanostructures during transit through the digestive tract, which could in turn be associated with changes in their toxicological effect [16]. In this work, the evaluation of two parameters representing animal viability were conducted, namely egg laying and motility.

Our experiment showed that exposure to high concentrations of magnetic composites (up to 100 µg/mL) does not reduce animal viability. At the highest concentration tested (500 µg/mL), only the bare MG nanoparticles exerted a detrimental effect in locomotion as well as in progeny. It was previously reported that high concentrations of iron affect *C. elegans* survival. The LD_{50} of acute exposure to iron was determined in 1.2 mM for *C. elegans*. It was also observed that sub-lethal iron concentrations decreased locomotor activity and brood size [21]. The mechanisms proposed for iron toxicity are associated to an increase in reactive oxygen species [34]. In this respect, the effects of nano-MG observed at the highest concentration administered on locomotion and progeny are directly associated to iron exposition. The iron concentration achieved at this dose for all magnetic compounds (Table S1) was above the LD_{50} reported in previous research [21], so the observed deleterious effects could be attributed to an iron excess. However, low viability is only observed in bare MNPs.

Previous studies demonstrated that the exposure of *C. elegans* to toxic iron concentrations may involve neuron damage, leading to changes in movement [24]. The decline in progeny associated to high levels of iron in *C. elegans* is related to a possible disruption of the cholinergic system, affecting egg-laying and progeny [24]. To correlate the results found on the biological assays with the iron content of the MNPs evaluated, iron was determined in NP aqueous dispersions (Table S1). Taken together, the results obtained show that functionalization of nano-MG, even with only OA, minimizes direct iron exposure and therefore diminishes the toxic effects associated to oxidative stress.

As far as authors' knowledge is concerned, only a few studies involving *C. elegans* as a model to evaluate toxicity of nanocompounds have been conducted to date. The first study was carried out by Kim et al. [35] who focused their work on the evaluation of silver NPs toxicity and found that bare NPs (100 µg/mL) and citrate-coated silver NPs (10 µg/mL) exert a deleterious effect on viability and reproduction. Gonzalez-Moragas et al. [15] studied *C. elegans* as an effective living model for the study of NPs toxicology and reported the protective effect of coating with bovine serum albumin on MNPs. In agreement with our results, these authors found that doses lower than 500 µg/mL affect significantly the animal viability and reported a protective effect due to coating.

The study of the cytotoxicity of nanocompounds is, in general, limited to the use of transformed cell lines. The metabolism of healthy cells is rather different from that of transformed cell lines. For example, major differences were

found in the toxicity of inorganic tellurite on freshly isolated peripheral blood leukocytes and in human chronic myeloid leukemia cell lines [35]. Specially, the studies on the cytotoxicity of magnetic nanosystems coated or functionalized with βCD are all based on in vitro experiments in tumor cell cultures, namely human cervical cancer cells (HeLa) [6, 7] human breast cancer cell lines (MDA-MB-231) [7], and human epidermoid carcinoma cells (A431) [8]. In order to evaluate the effect of βCD attaching on healthy mammalian cells, biocompatibility study was carried out in primary cultures of ECs, thus avoiding alteration in the results derived from the use of transformed cell lines. ECs, whose function is to regulate the exchange of biomolecules between bloodstream and surrounding tissues, were chosen taking into account that they form a single layer lining the entire vascular system. After administration, nanocompounds enter in direct contact with ECs to reach tissues and organs. The evaluation of the effect of βCD coating on ECs, in comparison to bare magnetite, is mandatory to ensure vascular biocompatibility of nanosystems as preliminary evaluation to ensure applicability of the nanosystem.

MTT is commonly used to evaluate cell viability because only living cells can reduce MTT to formazan. The latter can be spectrophotometrically quantified and is therefore a good cell-health parameter. The information obtained from this assay can be considered an indicator of cell health [34]. No effect on cell viability was detected until 100 µg/mL of the nanodevice in comparison to control cells. Only the cells exposed to 500 µg/mL MG@OA-βCD2 exhibited a decrease in viability evaluated by MTT assay. Still, the comparison of bare MG with the control revealed that a concentration of 100 µg/mL was already cytotoxic. Therefore, biocompatibility is strongly increased (around five-fold) upon βCD coating.

The biological results found in this work can be considered as pioneering advances about the impact of βCD coating on the toxicology of iron oxide nanoparticles. The high conservation of genes and signaling pathways between *C. elegans* and mammals and the use of rat aortic ECs represent the first stages for medical implementation of these nanosystems. The establishment of the biocompatible doses found in this work lay the groundwork for continuing clinical studies to ensure the implementation of these nanosystems in the biomedical applications mentioned, such as image contrast agents or drug transporters.

6 Conclusions

β-cyclodextrin (βCD) was successfully attached to oleic acid (OA)-coated magnetite (MG) nanoparticles. The novelty of the synthesis procedure here described ed lies in the manner of grafting the CDs to the magnetic component. The mechanism involved for coating, elucidated by an exhaustive analysis of the physicochemical properties, was based on the interactions between OA from functionalized MNPs and βCD through hosting. The physicochemical characteristics of the nanosystems obtained depends on the initial MG:βCD ratios. An optimum nanosystem in terms of size and surface charge was obtained with promising features as a magnetic nanocarrier for applications in biomedicine. The effect of βCD coating on the increment of biocompatibility in comparison to bare MG was studied. The assays performed on *C. elegans* as animal model and on healthy ECs revealed a positive impact of βCD coating on biocompatibility of MNPs. Taken together, our data confirm the key role of βCD coating in assuring the required biocompatibility to in vivo application of MNPs. Future insights regarding the nanosystems herein presented lie in ongoing with studies related to drug loading. The aim of this approach is to increase the specificity of nanoparticle-based medical treatments by improving drug localization.

Acknowledgements Authors thank Dr Diego Rayes for his kind support during the assays on *C. elegans*. This work was supported by "Consejo Nacional de Investigaciones Científicas y Técnicas" (CONICET) and "Universidad Nacional del Sur" (UNS).

Compliance with ethical standards

Conflict of interest The authors declare that they have no conflict of interest.

References

1. Mehta RV. Synthesis of magnetic nanoparticles and their dispersions with special reference to applications in biomedicine and biotechnology. Mater Sci Eng C. 2017;79:901–16.
2. Bakhtiary Z, Saei A, Hajipour MJ, Raoufi M, Vermesh O, Mahmoudi M. Targeted superparamagnetic iron oxide nanoparticles for early detection of cancer: possibilities and challenges. Nanomedicine. 2016;12:287–307.
3. Das P, Colombo M, Prosperi D. Recent advances in magnetic fluid hyperthermia for cancer therapy. Colloids Surf B. 2018;174:42–55.
4. Schneider MGM, Martin MJ, Coral D, Muraca D, Gentili C, van Raap MF, et al. Selective contrast agents with potential to the earlier detection of tumors: Insights on synthetic pathways, physicochemical properties and performance in MRI assays. Colloids Surf B. 2018;170:470–8.
5. Kainz QM, Reiser O. Polymer- and dendrimer-coated magnetic nanoparticles as versatile supports for catalysts, scavengers, and reagents. Acc Chem Res. 2014;47:667–77.
6. Badruddoza AZM, Rahman MT, Ghosh S, Hossain MZ, Shi J, Hidajat K, et al. β-Cyclodextrin conjugated magnetic, fluorescent silica core-shell nanoparticles for biomedical applications. Carbohydr Polym. 2013;95:449–57.

7. Tarasi R, Khoobi M, Niknejad H, Ramazani A, Ma'Mani L, Bahadorikhalili S, et al. β-cyclodextrin functionalized poly (5-amidoisophthalicacid) grafted Fe3O4 magnetic nanoparticles: a novel biocompatible nanocomposite for targeted docetaxel delivery. J Magn Magn Mater. 2016;417:451–9.
8. Monteiro APF, Caminhas LD, Ardisson JD, Paniago R, Cortés ME. Magnetic nanoparticles coated with cyclodextrins and citrate for irinotecan delivery. Carbohydr Polym. 2017;163:1–9.
9. Oroujeni M, Kaboudin B, Xia W, Jönsson P, Ossipov D. Conjugation of cyclodextrin to magnetic Fe3O4 nanoparticles via polydopamine coating for drug delivery. Prog Org Coat. 2018;114:154–61.
10. Zhou Y, Sun L, Wang H, Liang W, Yang J, Wang L. Investigation on the uptake and release ability of β-cyclodextrin functionalized Fe3O4 magnetic nanoparticles by methylene blue. Mater Chem Phys. 2016;170:83–89.
11. Santos ECS, Watanabe A, Vargas MD, Tanaka MN, Garcia F, Ronconi CM. AMF-responsive doxorubicin loaded β-cyclodextrin-decorated superparamagnetic nanoparticles. N J Chem. 2018;42:671–80.
12. Tarasi R, Khoobi M, Niknejad H, Ramazani A, Ma'Mani L, Bahadorikhalili S, et al. Beta-cyclodextrin functionalized poly (5-amidoisophthalicacid) grafted Fe3O4 magnetic nanoparticles: a novel biocompatible nanocomposite for targeted docetaxel delivery. J Magn Magn Mater. 2016;417:451–9.
13. Hunt PR. The *C. elegans* model in toxicity testing. Appl Toxicol. 2017;37:50–59.
14. Xiong H, Pears C, Woollard A. An enhanced *C. elegans* based platform for toxicity assessment. Sci Rep. 2017;7:1–11.
15. Gonzalez-Moragas L, Yu SM, Carenza E, Laromaine A, Roig A. Protective effects of bovine serum albumin on superparamagnetic iron oxide nanoparticles evaluated in the nematode caenorhabditis elegans. ACS Biomater Sci Eng. 2015;1:1129–38.
16. Gonzalez-Moragas L, Berto P, Vilches C, Quidant R, Kolovou A, Santarella-Mellwig R, et al. In vivo testing of gold nanoparticles using the *Caenorhabditis elegans* model organism. Acta Biomater. 2017;53:598–609.
17. Rayes D, Hernando G, Flamini M, Bouzat C. *Caenorhabditis elegans* muscle Cys-loop receptors as novel targets of terpenoids with potential anthelmintic activity. Mol Pharmacol. 2007;71:1407–15.
18. Stiernagle T. Maintenance of *C. elegans*, WormBook. New York, United States: Oxford University Press Inc.; 2006.
19. Committee for the Update of the Guide for the Care and Use of Laboratory Animals. Guide for the care and use of laboratory animals. 8th ed; Santiago, Chile: Ediciones Universidad Católica de Chile; 2011.
20. Issa B, Obaidat IM, Albiss BA, Haik Y. Magnetic nanoparticles: surface effects and properties related to biomedicine applications. Int J Mol Sci. 2013;14:21266–305.
21. Buckingham SD, Sattelle DB. Fast, automated measurement of nematode swimming (thrashing) without morphometry. BMC Neurosci. 2009;10:1–6.
22. Laura MD, Herndon A, Schmeissner PJ, Dudaronek JM, Brown PA, Listner KM, et al. Stochastic and genetic factors influence tissue-specific decline in ageing *C. elegans*. Nature. 2002;419:808–14.
23. De Almeida Fagundez D, Freitas Câmara D, Goulart Salgueiro W, Noremberg S, Puntel RL, Escobar Piccoli J, et al. Behavioral and dopaminergic damage induced by acute iron toxicity in *Caenorhabditis elegans*. Toxicol Res. 2015;4:878–84.
24. Mahoney TR, Luo S, Nonet ML. Analysis of synaptic transmission in *Caenorhabditis elegans* using an aldicarb-sensitivity assay. Nat Protoc. 2006;1:1772–7.
25. Zhang L, He R, Gu HC. Oleic acid coating on the monodisperse magnetite nanoparticles. Appl Surf Sci. 2006;253:2611–7.
26. Nakamoto K. Infrared and Raman Spectra of Inorganic and Coordination Complexes, Part B. New York: John Wiley and Sons Inc; 1997.
27. Vidal-Vidal J, Rivas J, López-Quintela Ma. Synthesis of monodisperse maghemite nanoparticles by the microemulsion method. Coll Surf A Physicochem Eng Asp. 2006;288:44–51.
28. Sambasevam KP, Mohamad S, Sarih NM, Ismail NA. Synthesis and characterization of the inclusion complex of β-cyclodextrin and Azomethine. Int J Mol Sci. 2013;14:3671–82.
29. Salustio PJ, Feio G, Figueirinhas JL, Pinto JF, Marques HMC. The influence of the preparation methods on the inclusion of model drugs in a beta-cyclodextrin cavity. Eur J Pharm Biopharm. 2009;71:377–86.
30. Kuo CH, Liu YC, Chang CMJ, Chen JH, Chang C, Shieh CJ. Optimum conditions for lipase immobilization on chitosan-coated Fe3O4 nanoparticles. Carbohydr Polym. 2012;87:2538–45.
31. Kaiser R, Miskolczy G. Magnetic properties of stable dispersions of subdomain magnetite particles. J Appl Phys. 1970; 41:1064–72.
32. Nicolás P, Saleta M, Troiani H, Zysler R, Lassalle V, Ferreira ML. Preparation of iron oxide nanoparticles stabilized with biomolecules: experimental and mechanistic issues. Acta Biomater. 2013;9:4754–62.
33. Anderson GL, Cole RD, Williams PL. Assessing behavioral toxicity with *Caenorhabditis elegans*. Environ Toxicol Chem. 2004;23:1235–40.
34. Mosmann T. Rapid colorimetric assay for cellular growth and survival: application to proliferation and cytotoxicity assays. J Immunol Methods. 1983;65:55–63.
35. Sandoval JM, Levêque P, Gallez B, Vásquez CC, Buc Calderon P. Tellurite-induced oxidative stress leads to cell death of murine hepatocarcinoma cells. Biometals. 2010;23(4):623–32.